

Article

In Vitro Cytotoxicity and *In Silico* Drug-Likeness of Secondary Metabolites from Endophytic *Aspergillus* spp. Isolated from *Brownlowia tersa*

Md. Mustafizur Rahman¹, Raiyan Rahman Reon^{1,*}, Partha Chandra Debnathe², Anike Chakrabarty³, and Md. Amirul Islam^{1,4,*}

¹ Pharmacy Discipline, School of Life Sciences, Khulna University, Khulna 9208, Bangladesh

² Department of Pharmacy, Noakhali Science and Technology University, Noakhali 3814, Bangladesh

³ Khulna Medical College Hospital, Khulna 9000, Bangladesh

⁴ Department of Pharmacy, East West University, Dhaka 1212, Bangladesh

* Correspondence: drzreon@gmail.com (R.R.R.); ma.islam@pharm.ku.ac.bd (M.A.I.)

Received: 30 January 2026; Revised: 24 March 2026; Accepted: 25 March 2026; Published: 30 March 2026

Abstract: Background: Mangrove-associated endophytic fungi are prolific producers of bioactive secondary metabolites with promising therapeutic applications. *Brownlowia tersa*, a medicinal mangrove species, harbors fungal endophytes that remain largely unexplored for their pharmacological potential. Objective: This study aimed to isolate endophytic fungi from *B. tersa*, characterize their secondary metabolites, and evaluate their cytotoxic, antibacterial, and antioxidant potentials through in vitro and silico approaches. Methods: Endophytic fungi were isolated from *B. tersa* leaves collected from the Sundarbans and identified morphologically and through ITS rDNA sequencing. Fungal crude extracts were screened for cytotoxicity against MCF-7 and SK-LU-1 human cancer cell lines using the SRB assay. Bioactive compounds were subjected to drug-likeness analysis via Lipinski's Rule of Five. Molecular docking was performed to assess the binding affinity of compounds previously reported in these species against bacterial DNA gyrase (GyrB) and the antioxidant enzyme Cu/Zn-SOD using AutoDock Vina. Results: Four *Aspergillus* species were isolated, among which *Aspergillus fumigatus* extracts (BTL-1, BTS-2) exhibited strong cytotoxic activity with IC₅₀ values of 17.06 ± 0.58 µg/mL and 14.35 ± 0.32 µg/mL. Chlorogenic acid, ar-turmerone, and lupenol were identified as promising compounds. Chlorogenic acid showed the highest docking affinities against GyrB (−8.1 kcal/mol) and Cu/Zn-SOD (−5.7 kcal/mol), with multiple stable hydrogen bonds, indicating strong antibacterial and antioxidant potential. Conclusion: The study highlights the therapeutic potential of *B. tersa*-associated endophytic fungi, particularly *Aspergillus fumigatus*, as a source of multi-target bioactive metabolites. Chlorogenic acid emerged as a promising lead for further development. These findings warrant subsequent in vivo validation and lead optimization for drug development.

Keywords: *Brownlowia tersa*; *Aspergillus fumigatus*; endophytic fungi; antioxidant; chlorogenic acid; molecular docking; cytotoxicity; mangrove; natural product

1. Introduction

Endophytes are microorganisms (fungi, bacteria, archaea, protists) that live inside plant tissues without causing immediate harm. They often form beneficial or neutral relationships influenced by host and environmental factors [1,2].

Mangrove plants have proven to be a rich source of endosymbiotic fungi, as shown by the large variety of fungal species isolated from them and the diverse bioactive compounds these fungi produce [3]. Mangrove trees provide ideal habitats for fungal symbionts. Endophytic fungi from mangroves produce diverse secondary metabolites with unique structures and bioactivities, supported by rich metabolic pathways and adaptive mechanisms [4]. *B. tersa* (Tiliaceae), native to tropical Asia, including the Sundarbans, has traditional uses against diarrhea, dysentery, wounds, and boils [5]. It exhibits strong antibacterial, antinociceptive, antidiarrheal, anti-allergic, and anti-hyperglycemic activities [6]. Phytochemical analyses of *B. tersa* ethanolic leaf extract revealed tannins, flavonoids, glycosides, saponins, reducing sugars, alkaloids, and carbohydrates. Notably, lignan carinol and 2'-hydroxyl acetophenone have been isolated from the plant [7].



Copyright: © 2026 by the authors. This is an open access article under the terms and conditions of the Creative Commons Attribution (CC BY) license (<https://creativecommons.org/licenses/by/4.0/>).

Publisher's Note: Scilight stays neutral with regard to jurisdictional claims in published maps and institutional affiliations.

In the last 10 years, around 600 endophytes with the potential to synthesize active compounds with therapeutic values have been isolated and cultivated in the laboratory [8,9]. Additionally, endophytes that mimic the chemistry of their host plant and produce metabolites identical to it, such as paclitaxel (also known as Taxol), jasmonic acid, ginkgolide, azadirachtin, and so forth, have been discovered [10]. Leucinostatin A, isolated from the endophytic fungus *Acremonium* sp., which inhabits the European yew (*Taxus baccata*), exhibits anti-cancer activities and acts as a fungicide against *Pythium ultimum* [11]. Echinocandin A is a lipopeptide that comes from endophytic fungus *Cryptosporiopsis* sp. and *Pezicula* sp. that live in Scots pine (*Pinus sylvestris*) and European beech (*F. sylvatica*), respectively. It is antifungal against *Candida albicans* and *Saccharomyces cerevisiae* [12]. Mangrove-derived endophytic fungus, *Irpex hydnooides* is shown to have a significant cytotoxicity against the Hep2 cell line. The anticancer drug Taxol has been demonstrated to occur in many endophytic fungi belonging to the genera *Alternaria*, *Fusarium*, *Monochaetia*, *Pestalotia*, *Pestalotiopsis*, *Pithomyces*, and *Taxomyces* [13]. Based on this, the objective of our study is to isolate and identify endophytic fungal strains from *B. tersa* and evaluate their bioactivity to provide a suitable lead that may be utilized in the future to pursue a new line of investigation for antimicrobial and anticancer effect.

2. Materials and Methods

2.1. In Vitro Studies

2.1.1. Sample Collection and Isolation of Endophytic Fungi

B. tersa plants were collected from Karamjal, Sundarbans, with local guide assistance, ensuring no harm to natural resources. The thawed plant parts were washed with distilled water, cut (0.5 cm²), and surface sterilized using 75% ethanol (1 min), 0.5% sodium hypochlorite (3 min), and 75% ethanol (30 sec), followed by rinsing with sterile distilled water. After blotting (3–4 h), sterilized tissues were placed on Potato Dextrose Agar with 150 mg/L Chloramphenicol under UV laminar flow. For one to three weeks, the plates were incubated at room temperature until fungal growth was observed. Similar fungal colony morphology, color, and size indicated the same species. A small fungal sample was transferred to a new Potato Dextrose medium plate with Chloramphenicol to obtain a pure culture. The fungus was grown for 5–10 days before storage [14].

2.1.2. Slide Culture Preparation

A slide culture for fungi is prepared by placing a small PDA agar block on a sterile microscope slide, supported by a U-shaped glass rod inside a Petri dish. Fungal spores or mycelial fragments are inoculated around the sides of the agar block, and a sterile cover slip is placed on top. The setup is incubated at room temperature for 48 h in a humid environment to encourage fungal growth. After incubation, the slide is examined under a low-power microscope to observe hyphal growth and spore formation, with additional incubation if necessary for improved visualization. The isolates were carefully identified with their reference, with a review of 2–3 times. The identity of the isolated strains is denoted BTL1, BTL2, BTL3, and BTL4, all of which are from the genus *Aspergillus*. Molecular identification based on the internal transcribed spacers (ITS) Region [15].

2.1.3. Genomic DNA Isolation

Fungal cells (up to 10⁸) were harvested, centrifuged at 6000× g for 5 min, and resuspended in 600 μL of sorbitol buffer. Lyticase was added, and cells were incubated at 30 °C to form spheroplasts, which were then lysed using Buffer CL mixed by vortex. The sample was incubated at 60 °C until clear, and RNA was optionally degraded using RNase A. Protein was removed with 100 μL of Buffer PO, followed by centrifugation. For sample preparation, 400 μL of Buffer BD was added, and the mixture was transferred to a DG column. The sample was washed with Buffer W1 and Buffer W2, followed by final centrifugation to remove residual wash buffer. DNA is eluted with pre-heated Buffer BE or TE and collected after centrifugation. Genomic DNA isolation has been conducted with modifications based on published articles [16].

2.1.4. Agarose Gel Electrophoresis

Agarose gel electrophoresis was employed to estimate DNA concentration. A 1% agarose gel was prepared in 1X TAE buffer, and isolated DNA samples were loaded into the wells. DNA migration was induced by applying an electric field, with smaller fragments migrating faster toward the anode, allowing size-based separation. The size range of DNA that can be resolved with the highest clarity depends on the proportion of agarose in the gel. Staining with the intercalating dye ethidium bromide allowed for the visualization of DNA bands. Due to its

mutagenic properties, appropriate safety measures were followed for the use and disposal of the dye. Agarose Gel Electrophoresis has been implemented with modifications consistent with published articles [17].

2.1.5. Sanger Sequencing

The PCR products were purified using a DNA purification reagent (Sigma-Aldrich, St. Louis, MI, USA) prior to sequencing. The purified DNA was subjected to Sanger sequencing by mixing the template DNA with sequencing primers, DNA polymerase, and deoxynucleotide triphosphates (dATP, dTTP, dGTP, and dCTP), along with a smaller proportion of fluorescent dye-labeled dideoxynucleotide triphosphates. During the sequencing reaction, the DNA template was initially denatured, followed by primer annealing and extension by DNA polymerase. Incorporation of a dideoxynucleotide resulted in chain termination, generating DNA fragments of varying lengths. These fragments were separated by capillary gel electrophoresis, where shorter fragments migrated faster through the gel matrix. As the fragments passed the detection point, a laser excited the fluorescent dyes attached to the terminal nucleotides, allowing the sequence to be determined based on the emitted fluorescence signals. The nucleotide sequence of the original DNA template was then reconstructed from the chromatogram generated by the fluorescence peaks [18].

Molecular identification of the fungal isolates was performed based on ITS rDNA sequence analysis. The obtained sequences were compared with reference sequences available in GenBank using BLAST analysis. The results indicated that isolates BTS-2, BTS-1, and BTL-1 exhibited high sequence similarity with *Aspergillus fumigatus*, whereas isolate BTL-2 showed close similarity to *Aspergillus flavus*. The sequences were deposited in GenBank under the accession numbers OP863036.1 (BTS-2), OP730546.1 (BTS-1), MH880190.1 (BTL-1), and OP480002.1 (BTL-2).

2.1.6. Extraction of Secondary Metabolites

Potato Dextrose Broth (PDB) was used to ferment the fungal stains. A fungal strain was cut into 1.5 cm pieces and transferred into a 500 mL Erlenmeyer flask containing 200 mL PDB. The flasks were incubated at room temperature under static and shaking conditions for three weeks. Cultures were filtered to remove mycelia, and the filtrate was defatted with *n*-hexane after incubation. After 2–4 h of ethyl acetate (1:1 v/v) extraction of fungal metabolites, crude extracts were evaporated and stored at 4 °C. Extraction of secondary metabolites is done according to the modified process mentioned in a research article [19].

2.1.7. Thin Layer Chromatography

A fine capillary tube was used to spot the fungal extract, and a minimal amount of fungal extract was taken in a small vial and diluted suitably with ethyl acetate. The sample was applied in uniform spots (~0.3 cm), several times to improve chromatogram quality, and each spot should dry before applying more. After spotting it, the solvent front was scratched, and the TLC plates were developed in a solvent system. The solvent system in the ratio of 1:1 (*n*-hexane and ethyl acetate) was kept in a jar. The plates were placed in the saturated jar with solvent just below the sample spots and allowed to run until the solvent traveled 7–8 cm. Plates were then air-dried, visualized under UV light for active compounds, and stained with potassium permanganate to reveal separate spots of compounds. After some modification, the TLC Process has been done according to a published article [20].

2.1.8. Cytotoxicity Assay

Cells were cultured, trypsinized with 0.25% trypsin, neutralized with FBS-containing medium, and counted using a hemocytometer with trypan blue. Cells were seeded at 2×10^4 (96-well) or 8×10^3 (384-well) per well. Treatment solutions were prepared in Opti-MEM or DMSO and added to wells (50 μ L in 96-well or 10 μ L in 384-well), followed by an equal volume of cell suspension. Plates included untreated, vehicle, and medium-only controls. After incubation at 37 °C in a CO₂ incubator, cells were fixed with 50% TCA (25 μ L or 5 μ L), incubated at 4 °C for 1 h, washed, dried, and stained with 0.04% SRB. Excess dye was removed with 1% acetic acid. Bound dye was solubilized with 10 mM Tris base (pH 10.5), and absorbance was read at 510 nm. % Cell growth = (Abs_{sample}/Abs_{control}) \times 100; % Inhibition = 100 – % Growth. Only OD values within the assay's linear range (≤ 2.0) were considered valid [21].

2.2. In-Silico Studies

2.2.1. Screening of the Compounds

Drug likeliness of isolated chemical compounds from *B. Tersa* was analyzed based on Lipinski's "rule of five", a widely accepted criterion for predicting oral bioavailability. The analysis was performed by the SwissAMDE web tool [22]. According to this rule, a compound is more likely to be orally active if it matches the following properties: molecular weight < 500 Da, hydrogen bond donors ≤ 5 , hydrogen bond acceptors ≤ 10 , and calculated LogP (cLogP) ≤ 5 . Compounds with a maximum of two violations of these parameters were taken into consideration for further research in this study.

2.2.2. Collection and Preparation of Ligands

Following the initial screening, the 3D conformers of a few selected chemical compounds were downloaded in SDF format from the PubChem chemical database [23]. Afterward, these 3D conformers were opened in Discovery Studio to add hydrogen atoms and clean the structure. Then the cleaned ligand structures were saved in PDB format for molecular docking and analysis. Ciprofloxacin and ascorbic acid were used as reference drugs for antibacterial and antioxidant activity.

2.2.3. Protein Selection and Preparation

The biological activity of selected phytochemicals was evaluated through molecular docking against both antibacterial and antioxidant targets. Protein targets were selected from representative Gram-positive (*Staphylococcus aureus*) and Gram-negative (*Escherichia coli*) bacterial strains to assess antibacterial potential. DNA gyrase subunit B (GyrB), a key enzyme involved in bacterial DNA replication, was selected as the molecular target due to its crucial role in ATP-dependent DNA supercoiling [24]. Specifically, Gyrase B (PDB ID: 4KFG) was selected as the target protein for G^{-ve} bacteria, while Gyrase B (PDB ID: 3TTZ) was used for G^{+ve} bacteria [25,26]. Copper, Zinc Superoxide Dismutase (Cu/Zn-SOD) was selected as the target protein for simulating antioxidant activity. This enzyme catalyzes the dismutation of superoxide radicals, which is essential for reducing oxidative stress.

The 3D crystal structures of GyrB from *E. coli* (PDB ID: 4KFG), *S. aureus* (PDB ID: 3TTZ), and Cu/Zn-SOD (PDB ID: 1CB4) were downloaded in PDB format from the RCSB Protein Data Bank [27]. The structures were then processed with BIOVIA Discovery Studio to exclude water molecules and other heteroatoms, and the file was saved in the (.pdb) format.

2.2.4. Molecular Docking and Visualization of Ligand–Receptor Interactions

Molecular docking was performed using PyRx version 0.8 with AutoDock Vina as the docking tool [9]. Before docking, the energy of all ligands was minimized and converted into the pdbqt format using PyRx 0.8's openbabel. After loading and converting the protein structures to macromolecules using AutoDock tools, molecular docking was carried out using AutoDock Vina. The docking grid was set to $26 \times 26 \times 26$ Å with a spacing of 1 Å, centered at $x = 38.202$, $y = 50.522$, and $z = 35.052$, and the exhaustiveness parameter was set to 32. The conformations with the least free binding energy (kcal/mol) were selected for post-docking analysis of ligand-protein interaction. Pymol (Schrodinger, LLC, New York, NY, USA), Discovery Studio (Accelrys Software Inc., San Diego, CA, USA), and Ligplot [28] were used to visualize the protein-ligand interaction. After docking, the results were exported as PyRx_AutoDock4.tar files containing the PDBQT files of receptors and ligands for further analysis. The receptor–ligand complexes were merged using PyMOL version 2.5.0 and saved in PDB format. The combined structures were then visualized in BIOVIA Discovery Studio 2021 to analyze 2D interactions and identify the specific amino acid residues involved in ligand binding [29].

3. Results

3.1. In Vitro Studies

Figure 1 illustrates the phylogenetic relationships of the isolated endophytic fungi based on ITS rDNA sequence analysis. The isolates were compared with reference sequences from GenBank to determine their taxonomic positions. BTS-1, BTS-2, and BTL-1 clustered closely with *Aspergillus fumigatus*, indicating a high degree of genetic similarity, whereas BTL-2 formed a separate clade associated with *Aspergillus flavus*. The clustering pattern was strongly supported by high bootstrap values obtained from 1000 replicates, confirming the reliability of the phylogenetic grouping. The scale bar (0.050) represents nucleotide substitutions per site, indicating the evolutionary distance among the sequences.

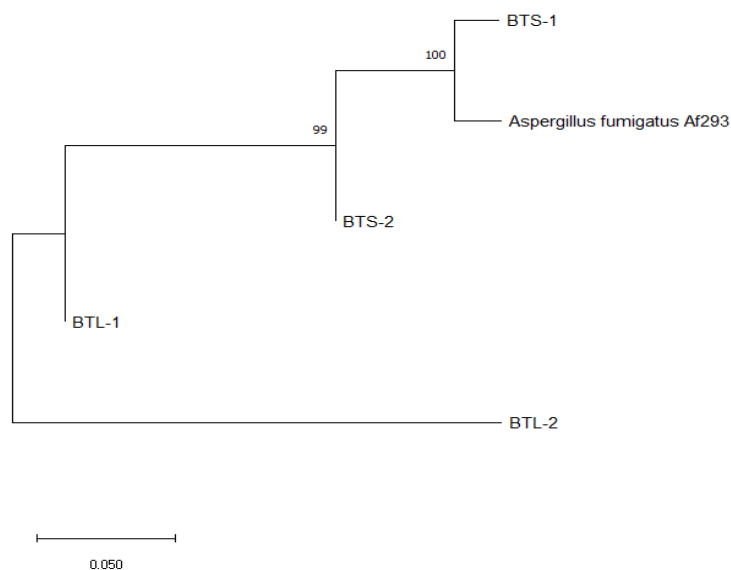


Figure 1. Phylogenetic evolutionary tree of promising endophytic isolates based on the ITS gene sequence (Bootstrap value 1000).

Tables 1 and 2 show cytotoxic IC_{50} values of endophytic fungal metabolites. The cytotoxic potential of metabolites from endophytic fungal isolates was evaluated against MCF-7 (breast) and SK-LU-1 (lung) adenocarcinoma cell lines. IC_{50} values, summarized in Table 1 for MCF-7 and Table 2 for SK-LU-1, reflect the inhibitory effects of these metabolites on cancer cell proliferation. All data are presented as mean \pm SEM.

All four endophytic fungal strains were initially screened using crude ethanolic extracts obtained through fermentation, followed by solvent extraction. The extracts were used directly in the biological assays without further fractionation. Although all strains were evaluated, only those demonstrating notable cytotoxic activity are presented in the tables for clarity.

Table 1 and Figure 2 present the cytotoxic potential of metabolites derived from two endophytic fungal strains, BTL-1 and BTS-2, against the human breast adenocarcinoma (MCF-7) cell line. Cytotoxicity was expressed as IC_{50} values ($\mu\text{g/mL}$), where lower values indicate higher potency. Among the tested strains, BTL-1 exhibited greater cytotoxic activity ($IC_{50} = 17.06 \pm 0.58 \mu\text{g/mL}$) compared to BTS-2 ($IC_{50} = 18.77 \pm 0.21 \mu\text{g/mL}$), indicating a relatively stronger inhibitory effect on MCF-7 cell proliferation.

Table 1. Cytotoxic IC_{50} values of endophytic fungal metabolites on Human Breast Adenocarcinoma (MCF-7) cell line.

Code of the Fungal Strains	IC_{50} Values ($\mu\text{g/mL}$)
BTL-1	17.06 ± 0.58
BTS-2	18.77 ± 0.21

All results presented here are with mean \pm SEM.

Table 2 and Figure 3 present the cytotoxic potential of metabolites derived from two endophytic fungal strains, BTL-1 and BTL-2, against the human lung adenocarcinoma (SK-LU-1) cell line. Cytotoxicity was expressed as IC_{50} values ($\mu\text{g/mL}$). Among the tested strains, BTL-1 demonstrated stronger cytotoxic activity ($IC_{50} = 14.35 \pm 0.32 \mu\text{g/mL}$) compared to BTL-2 ($IC_{50} = 18.09 \pm 0.09 \mu\text{g/mL}$), indicating a more effective inhibition of SK-LU-1 cell proliferation. These results suggest that BTL-1 metabolites could be considered a more promising candidate for further investigation as potential anticancer agents.

Table 2. Cytotoxic IC_{50} values of endophytic fungal metabolites on Human Lung Adenocarcinoma (SK-LU-1) cell line.

Code of the Fungal Strains	IC_{50} Values ($\mu\text{g/mL}$)
BTL-1	14.35 ± 0.32
BTL-2	18.09 ± 0.09

All results presented here with mean \pm SEM.

Sulforhodamine B (SRB) colorimetric cytotoxic assay on MCF-7 cell line

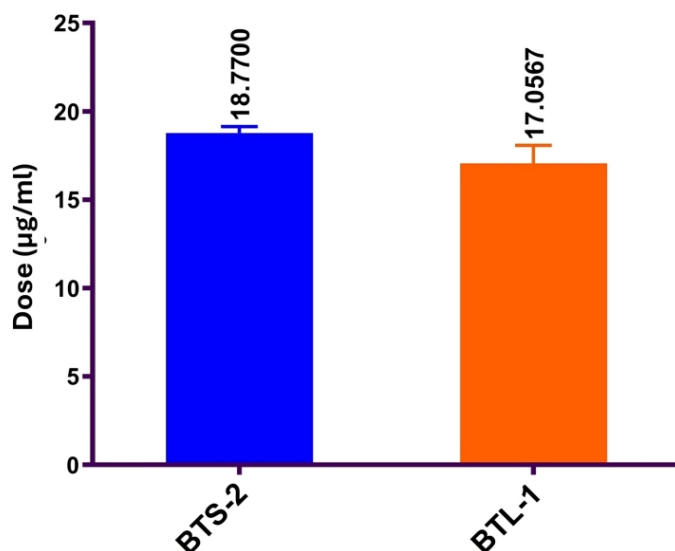


Figure 2. SRB colorimetric cytotoxic assay on MCF-7 cell line.

Sulforhodamine B (SRB) colorimetric cytotoxic assay on SK-LU-1 cell line

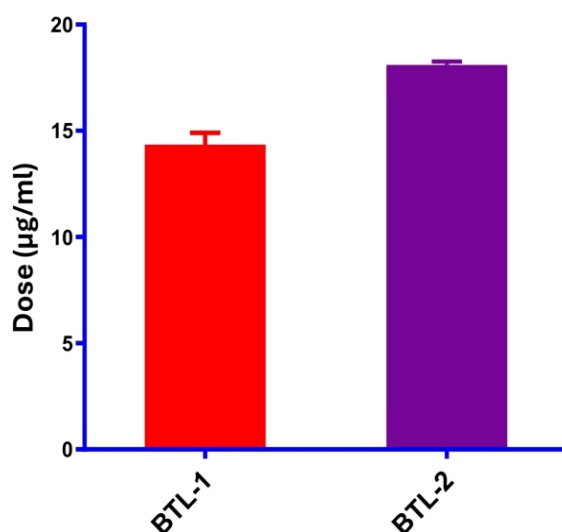


Figure 3. Graphical representation of cytotoxic IC₅₀ values of endophytic fungal metabolites on Human Lung Adenocarcinoma (SK-LU-1) cell line.

3.2. In Silico Findings

3.2.1. Drug-Likeness Screening

Drug-likeness is a key parameter in early-stage drug discovery, reflecting how “drug-like” a compound is in terms of its physicochemical properties, which influence absorption, distribution, metabolism, and excretion (ADME). In this study, drug-likeness was evaluated using Lipinski’s Rule of Five to predict the oral bioavailability of the isolated phytochemicals [30].

Among the tested compounds of Table 3, several compounds exhibited favorable drug-likeness profiles under Lipinski’s Rule of Five. Notably, chlorogenic acid, ar-turmerone, and lupenol showed promising physicochemical characteristics that align with drug-likeness parameters essential for oral bioavailability. Chlorogenic acid displayed a molecular weight of 354.31 Da, with 6 hydrogen bond donors and 9 acceptors, and a LogP value within the acceptable range, suggesting strong oral drug-like potential. Ar-turmerone, a bioactive compound derived from turmeric [31], exhibited a molecular weight of 216.32 Da, no hydrogen bond donors, only 1 hydrogen bond acceptor, and a LogP value of 3.24, fulfilling all four criteria of the rule and indicating good membrane permeability and solubility. Lupenol, a pentacyclic triterpenoid, had a higher molecular weight (426.72 Da) and a

LogP value of 8.02, which exceeds the recommended threshold. However, due to its known pharmacological activities [32] and compliance with other Lipinski parameters (0 hydrogen bond donors, 1 acceptor), it was retained for further analysis.

In contrast, several saturated hydrocarbons such as hentriacontane, triacontane, tetrapentacontane, and hexadecane showed significantly elevated LogP values (ranging from 8.28 to 28.86). This indicates poor aqueous solubility and low intestinal absorption, limiting their potential as orally active drugs. Overall, chlorogenic acid, ar-turmerone, and lupenol were considered suitable for further molecular docking studies based on their acceptable pharmacokinetic properties and compliance (complete or partial) with Lipinski's Rule of Five [29].

Table 3. Drug likeliness of selected chemical compounds.

Name	Molecular Weight	H-Bond Acceptors	H-Bond Donors	Consensus Log P
Chlorogenic Acid	354.31	09	06	-0.42
Ar-Turmerone	216.32	01	00	3.08
cis-2,4-Dimethylthiane, S, S-dioxide	162.25	02	00	1.32
Hentriacontane	436.84	00	00	16.41
Naphthalene	128.17	00	00	3.30
Hexadecane	226.44	00	00	8.28
Triacontane	422.81	00	00	15.87
2,4-Di-Tert-Butylphenol	206.32	01	01	5.19
Tetrapentacontane	759.45	00	00	28.86
Dotriacontane	450.87	00	00	16.95
Lupenol	426.729	01	01	8.0248
2-Methylhentriacontane	450.86	00	00	17.26
Eicosane,2,6,10,14,18-Pentamethyl	418	00	00	17.36
9-Octadecenamide	281.48	01	01	6.99

3.2.2. Molecular Docking and Visualization of Ligand–Receptor Interactions

Molecular docking studies were performed to evaluate the binding affinity of the selected phytochemicals (chlorogenic acid, ar-turmerone, and lupenol) against the antibacterial targets DNA gyrase subunit B (GyrB) from *E. coli* (PDB ID: 4KFG) and *S. aureus* (PDB ID: 3TTZ), as well as the antioxidant enzyme Cu/Zn-SOD (PDB ID: 1CB4). Ciprofloxacin and ascorbic acid were used as reference ligands for antibacterial and antioxidant docking, respectively.

Against GyrB (PDB ID: 4KFG) from Gram-negative bacteria, chlorogenic acid exhibited the highest binding affinity among the phytochemicals (Table 4 and Figure 4), with a docking score of -7.7 kcal/mol, forming six conventional hydrogen bonds with GLY117, VAL93, LEU94, and GLU42, as well as amide- π stacking interactions. Ar-turmerone and lupenol both had docking scores of -7.0 kcal/mol. Ar-turmerone interacted predominantly via hydrophobic contacts with ILE78, VAL43, and PRO79. Lupenol formed a conventional hydrogen bond with VAL93 and stabilized via multiple alkyl interactions. In comparison, the standard antibiotic ciprofloxacin (clinically established antibiotic) showed a docking score of -7.5 kcal/mol. Comparable docking score and binding interactions of chlorogenic acid highlight its potential antibacterial activity and validate the reliability of the molecular docking procedure used in this study.

For GyrB (PDB ID: 3TTZ) from Gram-positive bacteria, chlorogenic acid again demonstrated the strongest binding (Table 5 and Figure 5) among test compounds with a docking score of -8.1 kcal/mol, establishing hydrogen bonds with SER129, ASP81, ILE102, GLU50, and SER128. Ar-turmerone followed with -7.3 kcal/mol, forming hydrogen bonds with ARG84 and GLY85 and hydrophobic interactions with ILE86 and PRO87. Lupenol showed a docking score of -6.7 kcal/mol, primarily engaging through alkyl contacts. The reference compound ciprofloxacin had a binding energy of -8.0 kcal/mol, comparable to chlorogenic acid, reinforcing the phytochemical's antibacterial potential.

Docking with Cu/Zn-SOD (PDB ID: 1CB4) was carried out to evaluate antioxidant activity (Table 6 and Figure 6). Among the phytochemicals, only chlorogenic acid was docked, achieving a binding score of -5.7 kcal/mol. It has formed five conventional hydrogen bonds with GLY139, ARG141, and HIS78 and additional hydrophobic interactions with LYS134 and PRO60. The standard antioxidant ascorbic acid showed a slightly stronger binding energy of -6.4 kcal/mol, also forming multiple hydrogen bonds, confirming the reliability of the docking approach and supporting chlorogenic acid's antioxidant potential.

Overall, chlorogenic acid emerged as the most promising multi-target phytochemical, showing high binding affinities comparable to standard drugs. Ar-turmerone and lupenol also displayed meaningful interactions, particularly through hydrophobic contacts, indicating potential as antibacterial agents [33].

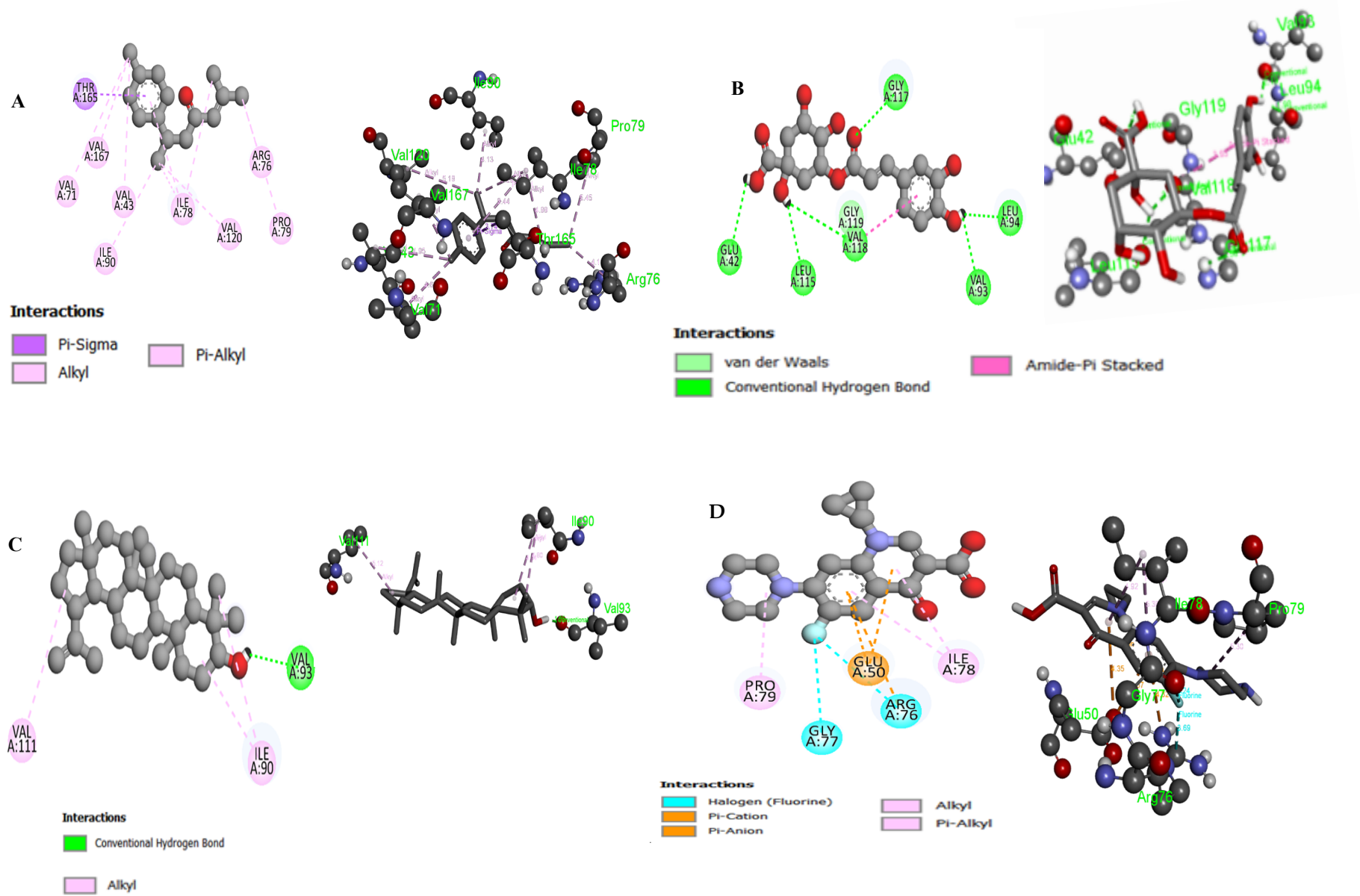


Figure 4. Interaction of 4KFG with ar-Turmerone (A); Chlorogenic acid (B); Lupen. ol (C); and Ciprofloxacin (D).

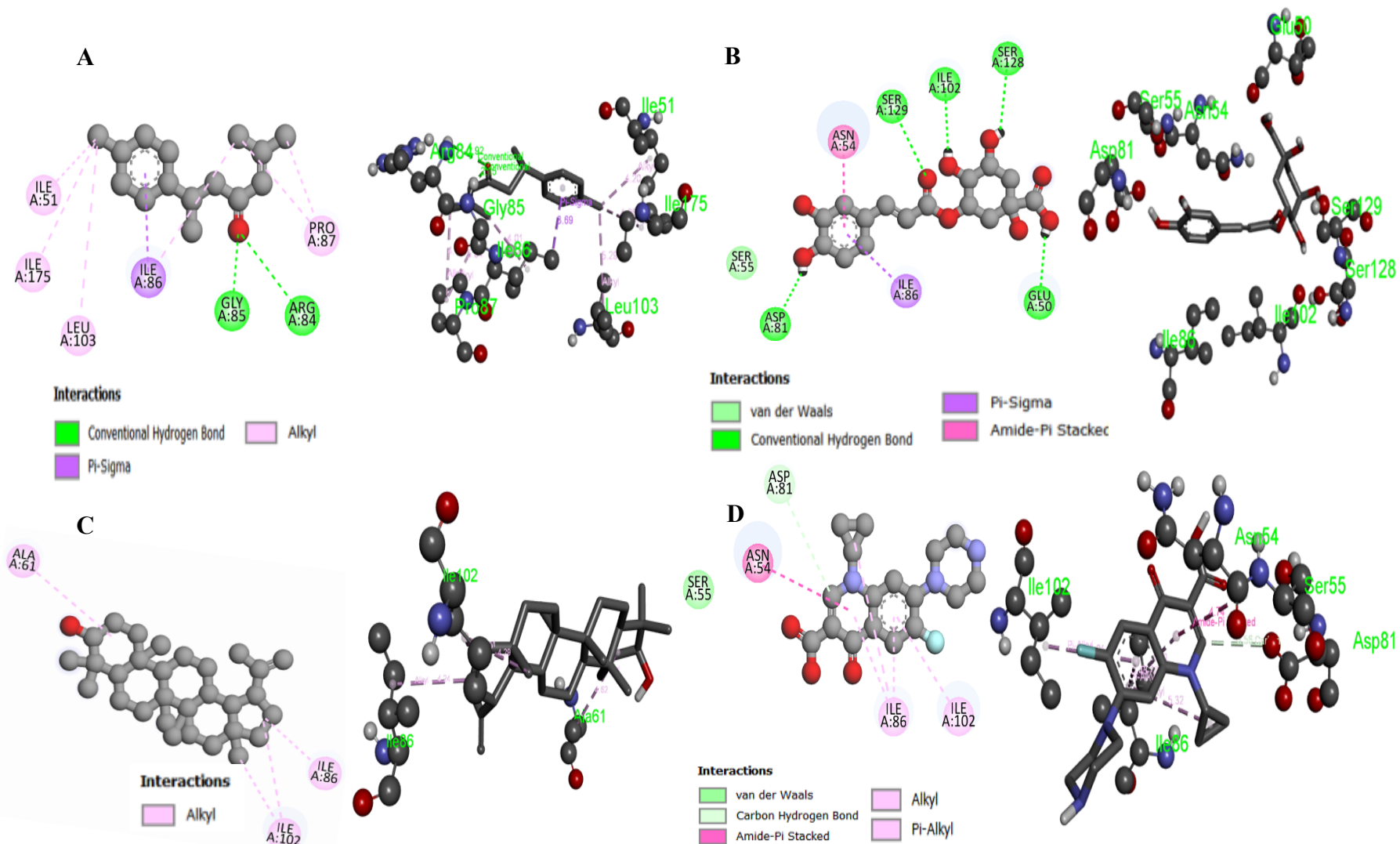


Figure 5. Interaction of 3TTZ with ar-Turmerone (A), Chlorogenic acid (B), Lupenol (C), and Ciprofloxacin (D).

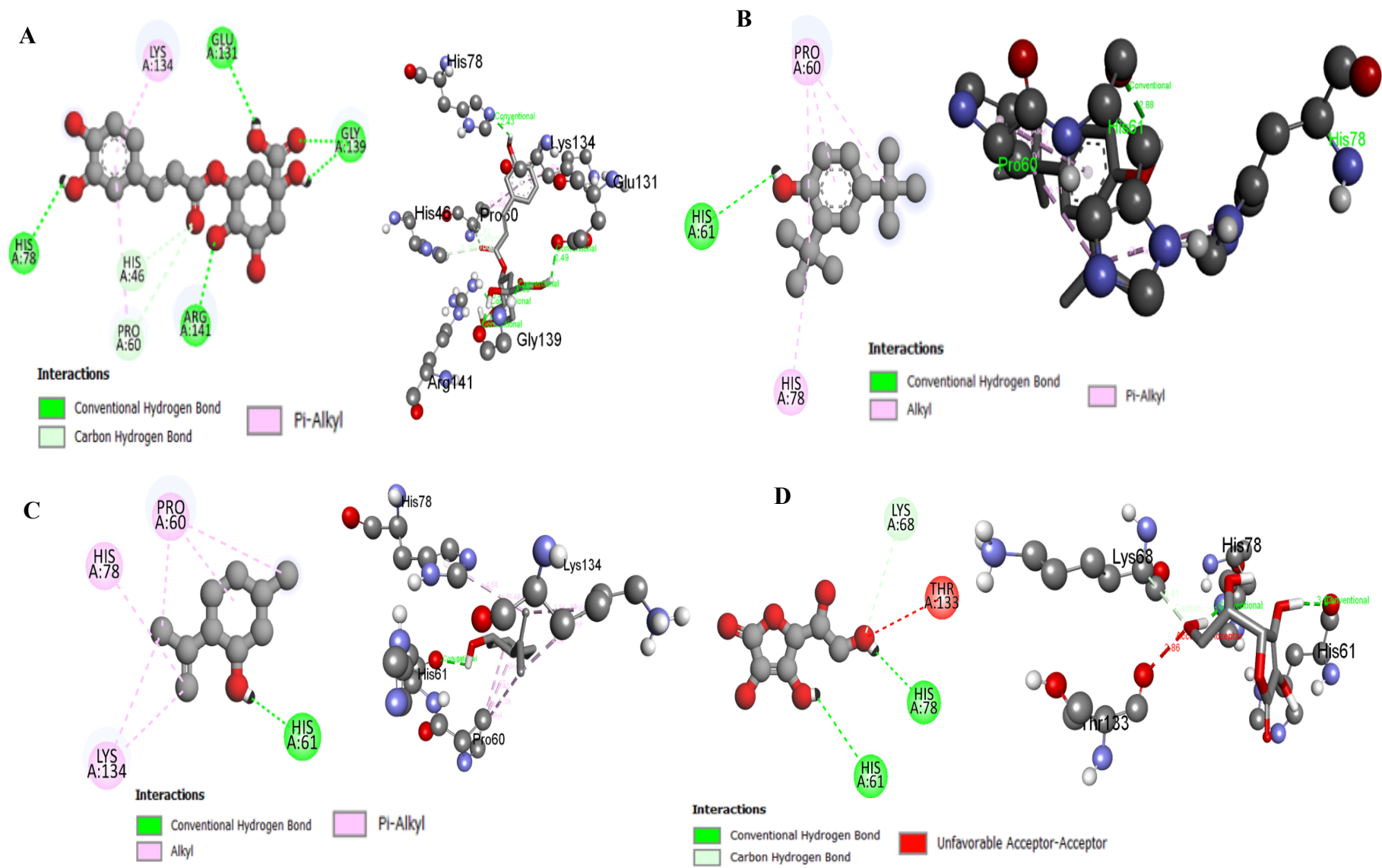


Figure 6. Interaction of 1CB4 with Chlorogenic acid (A), 2,4-Di-Tert-Butylphenol (B), Isopulegol (C), and Ascorbic acid (D).

Table 4. Molecular docking results of 4KFG with ar-Turmerone, Chlorogenic acid, Lupenol, and Ciprofloxacin.

L/N	Protein Name	Docking Score (kcal/mol)	Amino Acid	Distance	Other Categories of Interacting Bonds	Bond Types
Ar-Turmerone	4KFG	-7.0	THR165	3.74457	Pi-Sigma	(Hydrophobic)
			ILE78	4.2897	Alkyl	(Hydrophobic)
			ILE90	4.12803	Alkyl	(Hydrophobic)
			VAL120	5.18279	Alkyl	(Hydrophobic)
			ARG76	4.11025	Alkyl	(Hydrophobic)
			PRO79	5.44948	Alkyl	(Hydrophobic)
			ILE78	4.98595	Alkyl	(Hydrophobic)
			VAL43	4.95336	Alkyl	(Hydrophobic)
			VAL71	4.68718	Alkyl	(Hydrophobic)
			VAL167	4.18119	Alky	(Hydrophobic)
Chlorogenic acid	4KFG	-7.7	ILE78	5.43698	Pi-Alkyl	(Hydrophobic)
			GLY117	2.50351	Conventional Hydrogen Bond	(Hydrogen Bond)
			VAL93	2.19027	Conventional Hydrogen Bond	(Hydrogen Bond)
			LEU94	1.9785	Conventional Hydrogen Bond	(Hydrogen Bond)
			LEU115	2.43448	Conventional Hydrogen Bond	(Hydrogen Bond)
			VAL118	2.66971	Conventional Hydrogen Bond	(Hydrogen Bond)
			GLU42	2.58005	Conventional Hydrogen Bond	(Hydrogen Bond)
VAL118, GLY119	3.92915	Amide-Pi Stacked	(Hydrogen Bond)			
Lupenol	4KFG	-7.0	VAL93	1.9474	Conventional Hydrogen Bond	Hydrogen Bond
			VAL111	5.12148	Alkyl	Hydrophobic
			ILE90	4.63522	Alkyl	Hydrophobic
			ILE90	4.79761	Alkyl	Hydrophobic
Ciprofloxacin	4KFG	-7.5	ARG76	3.68738	Halogen (Fluorine)	Halogen
			GLY77	3.24471	Halogen (Fluorine)	Halogen
			ARG76	4.31978	Pi-Cation	Electrostatic
			GLU50	4.35078	Pi-Anion	Electrostatic
			GLU50	3.56591	Pi-Anion	Electrostatic
			PRO79	5.2991	Alkyl	Hydrophobic
			ILE78	4.91615	Pi-Alkyl	Hydrophobic
			ILE78	5.38421	Pi-Alkyl	Hydrophobic

Table 5. Molecular docking results of 3TTZ with ar-Turmerone, Chlorogenic acid, Lupenol, and Ciprofloxacin.

L/N	Protein Name	Docking Score (kcal/mol)	Amino Acid	Distance	Types of Interacting Bonds	Bond Category
Ar-Turmerone	3TTZ	-7.3	ARG84	2.91802	Conventional Hydrogen Bond	Hydrogen Bond
			GLY85	2.15302	Conventional Hydrogen Bond	Hydrogen Bond
			ILE86	3.69022	Pi-Sigma	Hydrophobic
			PRO87	4.56155	Alkyl	Hydrophobic
			ILE86	4.00834	Alkyl	Hydrophobic
			PRO87	5.03935	Alkyl	Hydrophobic
			ILE51	4.19966	Alkyl	Hydrophobic
			LEU103	5.28583	Alkyl	Hydrophobic
			ILE175	4.26104	Alkyl	Hydrophobic
			Chlorogenic acid	3TTZ	-8.1	SER129
ASP81	1.82268	Conventional Hydrogen Bond				Hydrogen Bond
ILE102	2.12216	Conventional Hydrogen Bond				Hydrogen Bond
GLU50	2.17807	Conventional Hydrogen Bond				Hydrogen Bond
GLU50	2.99711	Conventional Hydrogen Bond				Hydrogen Bond
SER128	2.6771	Conventional Hydrogen Bond				Hydrogen Bond
SER128	2.76191	Conventional Hydrogen Bond				Hydrogen Bond
ILE86	3.73008	Pi-Sigma				Hydrophobic
ASN54	4.96767	Amide-Pi Stacked	Hydrophobic			
Lupenol	3TTZ	-6.7	ALA61	4.6196	Alkyl	Hydrophobic
			ILE86	4.23522	Alkyl	Hydrophobic
			ILE102	4.82401	Alkyl	Hydrophobic
			ILE102	4.28758	Alkyl	Hydrophobic
Ciprofloxacin	3TTZ	-7.1	ASP81	3.56399	Carbon-Hydrogen Bond	Hydrogen Bond
			SER55	4.74276	Amide-Pi Stacked	Hydrophobic
			ILE86	5.32165	Alkyl	Hydrophobic
			ILE86	4.38977	Pi-Alkyl	Hydrophobic
			ILE86	4.43303	Pi-Alkyl	Hydrophobic
			ILE102	5.00525	Pi-Alkyl	Hydrophobic

Table 6. Molecular docking results of Super superoxide dismutase with ligands.

L/N	Protein Name	Docking Score (kcal/mol)	Amino Acid	Distance	Other Categories of Interacting Bonds	Bond Types
Cholorogenic acid	1CB4	-5.7	GLY139	1.88276	Conventional Hydrogen Bond	Hydrogen Bond
			ARG141	2.12592	Conventional Hydrogen Bond	Hydrogen Bond
			HIS78	2.42626	Conventional Hydrogen Bond	Hydrogen Bond
			GLY139	1.65813	Conventional Hydrogen Bond	Hydrogen Bond
			GLU131	2.48698	Carbon-Hydrogen Bond	Hydrogen Bond
			PRO60	3.33346	Pi-Alkyl	Hydrogen Bond
			PRO60	3.72365	Pi-Alkyl	Hydrogen Bond
			LYS134	5.44292	Pi-Alkyl	Pi-Alkyl
2,4-Di-Tert-Butylphenol	1CB4	-4.6	LYS134	4.17401	Pi-Alkyl	Pi-Alkyl
			HIS61	2.87906	Conventional Hydrogen Bond	Hydrogen Bond
			PRO60	5.11167	Alkyl	Hydrophobic
			PRO60	4.7561	Alkyl	Hydrophobic
			HIS78	5.11667	Pi-Alkyl	Hydrophobic
Isopulegol	1CB4	-4.5	PRO60	4.06231	Pi-Alkyl	Hydrophobic
			HIS61	2.51233	Conventional Hydrogen Bond	Hydrogen Bond
			PRO60	4.39935	Alkyl	Hydrophobic
			PRO60	5.07427	Alkyl	Hydrophobic
			PRO60	5.39104	Alkyl	Hydrophobic
			LYS134	4.23946	Alkyl	Hydrophobic
			LYS134	3.94411	Alkyl	Hydrophobic
Ascorbic acid	1CB4	-5.2	HIS78	4.57852	Pi-Alkyl	Hydrophobic
			HIS78	1.95791	Conventional Hydrogen Bond	Hydrogen Bond
			HIS61	3.03311	Conventional Hydrogen Bond	Hydrogen Bond
			LYS68	3.40561	Conventional Hydrogen Bond	Hydrogen Bond

4. Discussion

The present study adopted a multi-dimensional approach by integrating in vitro cytotoxic assays within in silico molecular docking and drug-likeness screening to evaluate the therapeutic potential of metabolites derived from endophytic fungi associated with *Brownlowia tersa*. While the observed results provide compelling evidence of bioactivity, it is essential to acknowledge that these findings remain incomplete without validation through in vivo experimentation.

In vivo models and in silico analysis would offer a more accurate representation of a compound's pharmacokinetics, pharmacodynamics, metabolism, toxicity, and systemic interactions, which are critical for determining its actual therapeutic viability [34,35]. In silico analysis was crucial for rapidly predicting the binding affinities and drug-likeness of fungal-derived compounds, helping to identify the most promising therapeutic leads. It minimized time and resource use by narrowing down candidates for future in vitro and in vivo validation [36].

Among the tested phytochemicals, chlorogenic acid emerged as the most promising compound. It consistently demonstrated high binding affinities across three significant biological targets—DNA gyrase subunit B of *E. coli* (PDB ID: 4KFG, docking score -7.7 kcal/mol), DNA gyrase of *S. aureus* (PDB ID: 3TTZ, -8.1 kcal/mol), and Cu/Zn-superoxide dismutase (PDB ID: 1CB4, -5.7 kcal/mol). These scores were comparable to standard antibacterial and antioxidant drugs like ciprofloxacin and ascorbic acid, respectively, suggesting strong inhibitory potential. Chlorogenic acid established multiple stable interactions, including hydrogen bonds and π -stacking with key amino acid residues, indicating favorable binding specificity and complex stability [37,38]. These in silico predictions were supported by the in vitro cytotoxic data, particularly for the *BTL-1* and *BTS-2* isolates, which exhibited low IC₅₀ values against MCF-7 and SK-LU-1 cancer cell lines, confirming their antiproliferative potential.

Other compounds, such as ar-turmerone and lupenol, also demonstrated notable binding profiles. Ar-turmerone interacted primarily via hydrophobic and π -alkyl bonds and met all parameters of Lipinski's Rule of Five, reinforcing its potential as an orally bioavailable compound [37]. On the other hand, lupenol, despite a high LogP value (8.02) indicating poor solubility, showed meaningful binding interactions through hydrophobic forces. Its inclusion in the study is justified by literature supporting its pharmacological relevance, including its anti-inflammatory and antibacterial effects [39].

One of the significant successes of this research lies in identifying multi-target compounds that exhibit both antibacterial and antioxidant properties. The docking models, validated by the use of standard ligands, and visualized using PyMOL and Discovery Studio, revealed that these phytochemicals establish specific and energetically favorable interactions with multiple receptor sites. This positions chlorogenic acid as a potential lead compound for further therapeutic exploration.

Moving forward, the logical next step would be to conduct in vivo studies using appropriate animal models to confirm the efficacy and safety profiles of the selected compounds. These studies would offer insight into the compounds' pharmacokinetics and toxicity, which are indispensable for therapeutic development. Simultaneously,

mechanistic investigations using molecular biology tools could shed light on the pathways modulated by these compounds, particularly those related to apoptosis, oxidative stress, and bacterial replication.

Further structural optimization, especially for hydrophobic compounds like lupenol, could enhance solubility and bioavailability. This may involve synthesizing derivatives or analogs with improved physicochemical properties. Additionally, ADME-Tox profiling and formulation studies, such as nanoencapsulation, could be used to improve the compounds' stability and targeted delivery. Lastly, combining these natural products with existing antibiotics or chemotherapeutic agents could be explored for synergistic effects, particularly in combating drug-resistant infections and cancers.

In conclusion, this study provides a strong foundation for the drug development potential of metabolites derived from mangrove endophytic fungi. Chlorogenic acid, ar-turmerone, and lupenol, in particular, demonstrated encouraging pharmacological profiles. With future *in vivo* validation and targeted modifications, these compounds could contribute meaningfully to the development of novel antibacterial, antioxidant, and anticancer agents [40].

Author Contributions: M.M.R., R.R.R. and M.A.I.: conceptualization; M.M.R. and M.A.I.: methodology, data curation; R.R.R., A.C. and M.M.R.: software; P.C.D., M.A.I. and R.R.R.: validation; A.C.: formal analysis; M.M.R.: investigation, resources; M.M.R., R.R.R., A.C. and P.C.D.: writing—original draft preparation; M.M.R., R.R.R., A.C. and P.C.D.: writing—review and editing; M.A.I. and M.M.R.: visualization; M.A.I.: supervision, project administration. All authors have read and agreed to the published version of the manuscript.

Funding: This research received no external funding.

Institutional Review Board Statement: Not applicable.

Informed Consent Statement: Not applicable.

Data Availability Statement: Not applicable.

Conflicts of Interest: The authors declare no conflict of interest.

Use of AI and AI-Assisted Technologies: During the preparation of this work, the authors used QuillBot and Grammarly for language editing and grammatical correction. After using these tools, the authors reviewed and edited the content as needed and took full responsibility for the content of the published article.

References

1. Noshin, S.; Bairagi, R.D.; Airin, S.; et al. *In Vitro* Activity of Isolated Bioactive Metabolites from Endophytic Fungus Associated with *Aegiceras corniculatum*. *J. Med. Nat. Prod.* **2025**, *2*, 100003.
2. Wilson, D. Endophyte: The Evolution of a Term, and Clarification of Its Use and Definition. *Oikos* **1995**, *74*, 274–276.
3. Hamzah, T.N.T.; Ozturk, M.; Altay, V.; et al. Insights into the Bioactive Compounds of Endophytic Fungi in Mangroves. In *Biodiversity and Biomedicine*; Academic Press: New York, NY, USA, 2020; pp. 277–292.
4. Deng, C.M.; Liu, S.X.; Huang, C.H.; et al. Secondary Metabolites of a Mangrove Endophytic Fungus *Aspergillus terreus* (No. GX7-3B) from the South China Sea. *Mar. Drugs* **2013**, *11*, 2616–2624.
5. Mannan, M.A. *Brownlowia tersa* (Linn.) Kosterm: A Review of Traditional Uses, Phytochemistry and Pharmacology. *Genus* **2019**, *7*, 34–37.
6. Chakrabarty, B.; Kundu, N.; Acharyya, R.N.; et al. Investigation of Anti-Hyperglycemic, Anti-Allergic Activities of Ethanolic Extract from *Brownlowia tersa* (L.) Stem. *J. Med. Plants Stud.* **2022**, *10*, 43–46.
7. Hossain, H.; Jahan, I.A.; Howlader, S.I.; et al. Anti-Inflammatory and Antioxidant Activities of Ethanolic Leaf Extract of *Brownlowia tersa* (L.) Kosterm. *Orient. Pharm. Exp. Med.* **2013**, *13*, 181–189.
8. Patil, R.H.; Patil, M.P.; Maheshwari, V.L. Bioactive Secondary Metabolites from Endophytic Fungi: A Review of Biotechnological Production and Their Potential Applications. *Stud. Nat. Prod. Chem.* **2016**, *49*, 189–205.
9. Elsarkasi, R.F.; Rabie, G.H.; El-Gazzar, N. Article Review on Bioactivity of Secondary Metabolites of Endophytic Fungi. *Bull. Fac. Sci. Zagazig Univ.* **2025**, *2025*, 243–251.
10. Burragoni, S.G.; Jeon, J. Applications of Endophytic Microbes in Agriculture, Biotechnology, Medicine, and Beyond. *Microbiol. Res.* **2021**, *245*, 126691.
11. Kawaratani, Y.; Matsuoka, T.; Hirata, Y.; et al. Influence of the Carbamate Fungicide Benomyl on the Gene Expression and Activity of Aromatase in the Human Breast Carcinoma Cell Line MCF-7. *Environ. Toxicol. Pharmacol.* **2015**, *39*, 292–299.
12. Denning, D.W. Echinocandins: A New Class of Antifungal. *J. Antimicrob. Chemother.* **2002**, *49*, 889–891.
13. Uzma, F.; Mohan, C.D.; Hashem, A.; et al. Endophytic Fungi—Alternative Sources of Cytotoxic Compounds: A Review. *Front. Pharmacol.* **2018**, *9*, 309.
14. Kamat, S.; Kumari, M.; Taritla, S.; et al. Endophytic Fungi of Marine Alga from Konkan Coast, India—A Rich Source of Bioactive Material. *Front. Mar. Sci.* **2020**, *7*, 31.
15. Harris, J.L. Modified Method for Fungal Slide Culture. *J. Clin. Microbiol.* **1986**, *24*, 460–461.

16. Michael, K.; Andreou, C.; Markou, A.; et al. A Novel Sorbitol-Based Flow Cytometry Buffer Is Effective for Genome Size Estimation across a Cypriot Grapevine Collection. *Plants* **2024**, *13*, 733.
17. Green, M.R.; Sambrook, J. Analysis of DNA by Agarose Gel Electrophoresis. *Cold Spring Harb. Protoc.* **2019**, 2019, pdb.top100388.
18. Nikezić, A.; Blagojević, S.; Čupurdija, M.; et al. Comparative Analysis of Human DNA Extraction Methods and Mitochondrial DNA HV1 and HV2 Haplogroup Determination. *Kragujevac J. Sci.* **2020**, *42*, 73–83.
19. Park, J.C.; Nemoto, Y.; Homma, T.; et al. Adaptation of *Aspergillus niger* to Several Antifungal Agents. *Microbiology* **1994**, *140*, 2409–2414.
20. Miyamoto, T. Thin Layer Chromatography. *Kobunshi* **1974**, *23*, 378–383.
21. Orellana, E.A.; Kasinski, A.L. Sulforhodamine B (SRB) Assay in Cell Culture to Investigate Cell Proliferation. *Bio-protocol* **2016**, *6*, e1984.
22. SwissADME. Available online: <http://www.swissadme.ch/> (accessed on 10 January 2025).
23. PubChem. Available online: <https://pubchem.ncbi.nlm.nih.gov/> (accessed on 9 January 2025).
24. Khan, T.; Sankhe, K.; Suvarna, V.; et al. DNA Gyrase Inhibitors: Progress and Synthesis of Potent Compounds as Antibacterial Agents. *Biomed. Pharmacother.* **2018**, *103*, 923–938.
25. Zeleke, D.; Eswaramoorthy, R.; Belay, Z.; et al. Synthesis and Antibacterial, Antioxidant, and Molecular Docking Analysis of Some Novel Quinoline Derivatives. *J. Chem.* **2020**, 2020, 1324096.
26. Grossman, S.; Fishwick, C.W.; McPhillie, M.J. Developments in Non-Intercalating Bacterial Topoisomerase Inhibitors: Allosteric and ATPase Inhibitors of DNA Gyrase and Topoisomerase IV. *Pharmaceuticals* **2023**, *16*, 261.
27. RCSB Protein Data Bank. Available online: <https://www.rcsb.org/> (accessed on 9 January 2025).
28. Wallace, A.C.; Laskowski, R.A.; Thornton, J.M. LIGPLOT: A Program to Generate Schematic Diagrams of Protein-Ligand Interactions. *Protein Eng. Des. Sel.* **1995**, *8*, 127–134.
29. Berkane, A.; Kundu, N.; Munia, A.A.; et al. Quercetin Derivatives as Potential Inhibitors of Nipah Virus Phosphoprotein through *in Silico* Drug Design Approaches. *J. Indian Chem. Soc.* **2024**, *101*, 101196.
30. Bitew, M.; Desalegn, T.; Demissie, T.B.; et al. Pharmacokinetics and Drug-Likeness of Antidiabetic Flavonoids: Molecular Docking and DFT Study. *PLoS ONE* **2021**, *16*, e0260853.
31. Takemoto, Y.; Sumi, T.; Kishi, C.; et al. Distribution of Inhaled Volatile Turmerones in the Mouse. *Food Biosci.* **2021**, *41*, 100965.
32. Siddique, H.R.; Saleem, M. Beneficial Health Effects of Lupeol Triterpene: A Review of Preclinical Studies. *Life Sci.* **2011**, *88*, 285–293.
33. Tasnim, N.; Chakrabarty, B.; Biswas, B.; et al. Exploration of Analgesic, Laxative and Immunomodulatory Effects of Leaves and Twigs of *Euphorbia tirucalli* along with *in Silico* Analysis. *J. Med. Plants Stud.* **2024**, *12*, 1–10.
34. Islam, M.R.; Sharma, S.; Arafat, S.Y.; et al. Identification of New Inhibitors for the Avian H1N1 Virus through Molecular Docking and Dynamic Simulation Approaches. *J. Indian Chem. Soc.* **2024**, *101*, 101274.
35. Uddin, M.B.; Praseetha, P.K.; Ahmed, R.; et al. Identification of Natural Compounds as Potential Antiviral Drug Candidates against Hepatitis E Virus through Molecular Docking and Dynamics Simulations. *J. Indian Chem. Soc.* **2024**, *101*, 101446.
36. Agbeniyi, O.T.; Kumar, N.; Kuthi, N.A.; et al. The Anti-Leukemic Activities of Campesterol and α -Tocopherol Against BCL-2 Target through Computational Drug Design Approaches. *Curr. Top. Med. Chem.* **2025**, *25*, 813–823.
37. Gurung, A.B.; Bhattacharjee, A.; Ali, M.A. Exploring the Physicochemical Profile and the Binding Patterns of Selected Novel Anticancer Himalayan Plant Derived Active Compounds with Macromolecular Targets. *Inform. Med. Unlocked* **2016**, *5*, 1–14.
38. Sanchez, M.B.; Miranda-Perez, E.; Verjan, J.C.G.; et al. Potential of the Chlorogenic Acid as Multitarget Agent: Insulin-Secretagogue and PPAR α/γ Dual Agonist. *Biomed. Pharmacother.* **2017**, *94*, 169–175.
39. Liu, K.; Zhang, X.; Xie, L.; et al. Lupeol and Its Derivatives as Anticancer and Anti-Inflammatory Agents: Molecular Mechanisms and Therapeutic Efficacy. *Pharmacol. Res.* **2021**, *164*, 105373.
40. Sohag, A.A.M.; Hossain, M.T.; Rahaman, M.A.; et al. Molecular Pharmacology and Therapeutic Advances of the Pentacyclic Triterpene Lupeol. *Phytomedicine* **2022**, *99*, 154012.